JOURNAL OF MATERIALS SCIENCE 22 (1987) 4541–4545

Porous materials prepared by heating derivatives from halloysite

ASAO ŌYA*, KAZUHISA KIZU, SUGIO ŌTANI
Faculty of Engineering, Gunma University, Kiryu, Gunma 376, Japan

Halloysite clay was subjected to serious treatment by trimethylsilylation and hydrochloric acid. The resulting derivatives were heated below 1473 K in nitrogen or air to prepare thermally stable porous materials including larger pores than those in zeolite. The trimethylsilylated halloysite resulted in a thermally stable porous material, in an amorphous state, including extremely uniform pores of 1.7 nm. Another derivative also resulted in a thermally stable porous material but consisted of very heterogeneous pores. The thermal degradation behaviour of both derivatives is discussed in detail.

1. Introduction

Halloysite (HA) is known to be converted into the trimethylsilyl derivative (TSH) as shown in Fig. 1 on treating with a mixture of hexamethyldisiloxane, *i*-propanol and hydrochloric acid [1]. In this figure, PTSH and CTSH indicate the TSH derivatives subjected to mild and serious trimethylsilylation treatments, respectively. We thought that TSH resulted in a thermally stable porous material after heating, consisting of an Si–O tetrahedron sheet cross-linked with an –Si–O– pillar. In fact, as reported earlier [2], a thermally stable porous material including extremely homogeneous pores of 1.7 nm was prepared from the PTSH. This aroused our interest in the preparation of porous materials from the other two derivatives from HA. They are the derivatives (CTSH and CHA in Fig. 1) subjected to serious trimethylsilylation and hydrochloric acid-treatment, respectively. The purposes of the present paper are (i) to clarify the thermal degradation behaviour of the derivatives, leading to the porous material, and (ii) to discuss properties of the porous material resulting from the CTSH.

2. Experimental details

2.1. Preparation and heat-treatment procedures

20 g raw HA (– 120 μm) (Indiana, USA) was treated with 260 ml hexamethyldisiloxane, 200 ml *i*-propanol and 200 ml 4 N-hydrochloric acid at 333 K for 10 days with stirring. Because the resulting material contained a little raw HA, it was subjected to further trimethylsilylation at 338 K for 3 days until HA disappeared completely. The CTSH was dried at 403 K after thorough washing with a water/*i*-propanol mixture. The preparation was repeated in a batchwise operation three times, and the total amount of resulting CTSH was 10.5 g from 60 g raw HA.

The CHA was prepared as follows; 30 g raw HA (– 120 μm) was reacted with 900 ml 4 N-hydrochloric acid at 333 K for 3 days until it disappeared completely. The CHA obtained weighed 9.1 g after washing with water and subsequent drying at 403 K. Both derivatives thus prepared were heated to a prefixed temperature between 473 and 1473 K at a heating rate of 5 K min^{-1} and held for 1 h in nitrogen and air.

2.2. Measurements

The carbon content of the CTSHs was measured by the combustion method using tin particles to aid combustion. X-ray powder diffraction using Cu$K\alpha$ radiation and infrared spectrum measurement were carried out according to the conventional methods. Thermogravimetric analysis was conducted at a heating rate of 10 K min^{-1} in a flow of nitrogen or air. BET specific surface area was measured using a nitrogen absorbent, and in addition, a pore-size distribution diagram was made using the Cranston–Inkley method. The acidic property was determined by thermogravimetric analysis using an NH_3 absorbent. As acidic strength and acidity increase, NH_3 is adsorbed on the sample in larger amounts and up to higher temperatures.

3. Results

3.1. X-ray diffraction analysis

Figs 2 and 3 show X-ray diffraction profiles of the CTSH and the CHA before and after heating in nitrogen. The CTSH remained in an amorphous state, until it crystallized into cristobalite (SiO_2) at 1473 K (Fig. 2). Similar phenomena were also observed in the CHA except for the appearance of a broad peak around 20° (2θ, Cu$K\alpha$) which could not be assigned (Fig. 3). The thermal behaviour of both samples in air was substantially the same as that in nitrogen (though not presented here). In view of the formation of mullite ($2\,SiO_2 \cdot 3\,Al_2O_3$) in raw HA and the PTSH after heating to 1473 K as reported in the previous paper [2], the CTSH and the CHA contain no or only a small amount of aluminium.

---

*Author to whom all correspondence should be addressed.

0022–2461/87 $03.00 + .12

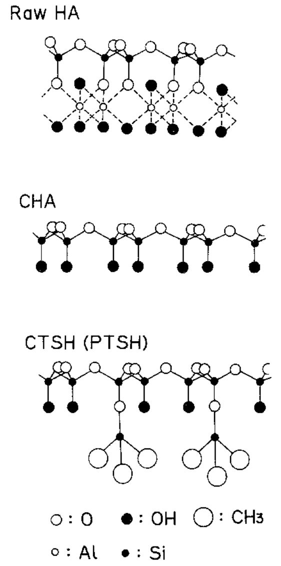

Figure 1 Schematic models of the structures of raw HA, CTSH(PTSH) and CHA.

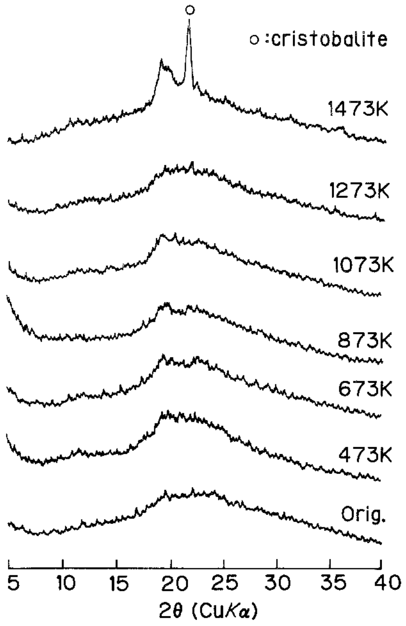

Figure 3 X-ray diffraction profiles of CHA before and after heating in nitrogen.

3.2. Infrared spectrum measurement

Fig. 4 shows the infrared spectra of CTSH and CHA. The spectrum of the CTSH is quite similar to that reported by Kuroda and Kato [1]. They assigned the absorptions as follows: 2960 cm^{-1} ν-CH$_3$; 1260 cm^{-1} δ-CH$_3$; 1050 to 90 cm^{-1} ν-Si–O–Si; 750 cm^{-1} ϱ-CH$_3$. These absorptions remained up to 873 K in nitrogen and to 673 K in air, respectively. The CHA exhibited two absorptions at 1630 and 3400 cm^{-1} assigned to –OH, which remained up to 1073 K in both atmospheres.

3.3. Thermogravimetric analysis

TG–DTA curves of CTSH and CHA in a flow of air are shown in Fig. 5. The CHA exhibited two weight decreases, without corresponding changes in the DTA curve, which possibly resulted from the removal of adsorbed water and dehydration from –OH. This behaviour was changed little on heating in nitrogen. The CTSH in air, on the other hand, exhibited two exothermic weight decreases around 700 and 800 K. These must be attributable to the combustion of CH$_3$ introduced. Such exothermic peaks did not appear for CTSH heated in nitrogen, but a weight decrease was observed at a temperature just slightly above 800 K (though not presented here). The final weight decrease at 1473 K was 14 wt %.

3.4. Carbon content

Table I shows the carbon contents of the CTSHs heated to various heat-treatment temperatures (HTT). The content of 16 wt % before heating remained unchanged up to 673 K in nitrogen and decreased to one-half at 873 K. The decrease continued at higher HTTs and reached 2 wt % at 1473 K. Under heat-treatment in air, on the other hand, the carbon content of the CTSH reduced to one-half at 673 K and was just

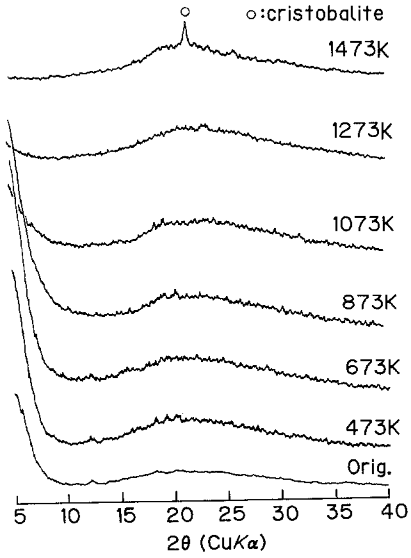

Figure 2 X-ray diffraction profiles of CTSH before and after heating in nitrogen.

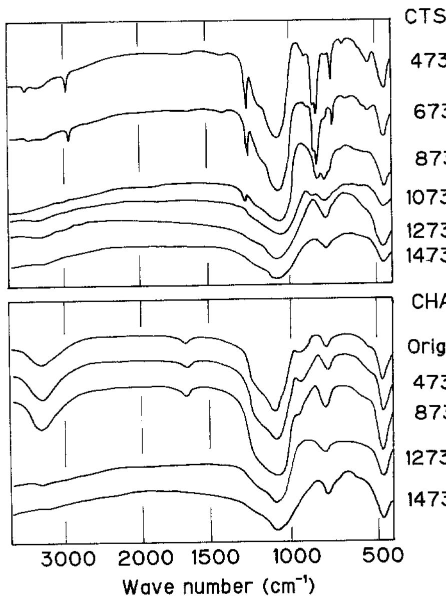

Figure 4 Infrared spectra of CTSH and CHA before and after heating in nitrogen.

TABLE I Carbon contents (wt %) of CTSH before and after heating in nitrogen and air

HTT (K)	Heat-treatment atmosphere	
	N_2	Air
Original	15.5	
473	17.3	17.8
673	15.7	7.9
873	8.6	0.9
1073	6.6	0.6
1273	5.4	0.2
1473	1.9	0.1

1 wt % at 873 K. A further decrease was observed at higher HTTs.

3.5. BET specific surface area

Table II summarizes the specific surface areas of CTSH, CHA together with PTSH reported previously [2]. The surface area of CHA was about 400 $m^2 g^{-1}$ up to 873 K and then decreased gradually with increasing HTT in both heat-treatment atmospheres. A large surface area (300 $m^2 g^{-1}$) was obtained even after heating to 1273 K. The crystallization of CHA into cristobalite at 1473 K brought about a steep decrease in the surface area.

The surface area of CTSH was influenced by the heat-treatment atmosphere. Its surface area, 500 $m^2 g^{-1}$, before heating increased to the maximum values of 750 $m^2 g^{-1}$ at 873 K in nitrogen and 650 $m^2 g^{-1}$ at 673 K in air, respectively. The nitrogen was more effective in retaining the large surface area up to high HTT. The surface areas of both CTSH and CHA are considerably larger than that of PTSH reported previously [2].

3.6. Pore-size distribution

Pore-size distribution diagrams of some samples are shown in Figs 6, 7 and 8. CHA before heating exhibited a broad distribution diagram with a small maximum peak at 1.7 nm. On the other hand, a narrow diagram with a sharp maximum at 1.7 nm was obtained for CTSH (Fig. 6). There was no difference between the diagrams of the CTSHs after heating to 873 K in both atmospheres, although the surface area was influenced by the atmosphere (Fig. 7). The atmosphere had no effect on the pore-size distribution of CHA (Fig. 8). The diagrams of CTSH and CHA were also little influenced by HTT.

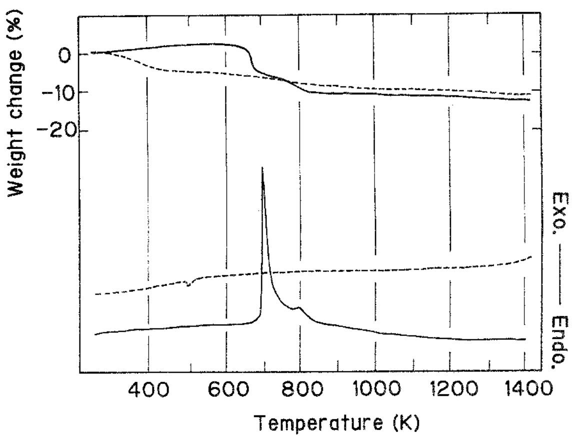

Figure 5 TG–DTA curves of (——) CTSH and (– – –) CHA, before heating in air.

3.7. Acidic property

Fig. 9 shows the TG data of some samples, including the commercially available catalysts, using an HN_3 absorbent. Zeolon (Norton Inc.) exhibited by far the most superior acidic property, both in acidic strength and acidity, compared to other samples. The acidic property of raw HA was very similar to that of N-631L (silica/alumina catalyst) and slightly superior to JRC-ALO-1 (alumina catalyst), but was lowered through the treatments used here. Comparison of the acidic properties of CTSH and CHA shows that the introduction of trimethylsilyl group had no favourable effect on the acidic property of the resulting porous material.

4. Discussion

4.1. Thermal degradation behaviour of CTSH

CTSH must have the structure shown in Fig. 1 in view of the following results: the appearance of absorptions assigned to $-CH_3$ (Fig. 4), the large exothermic weight decrease in air (Fig. 5) and the presence of no or only a little aluminium as suggested from the formation of cristobalite instead of mullite at 1473 K (Fig. 2). The resulting CTSH is in an amorphous state because the Si–O tetrahedron sheet is not sufficiently rigid to maintain a layer structure even when supported with trimethylsilyl pillar. When one-half and one-quarter of the groups in the CHA are trimethylsilylated, the carbon contents of the resulting derivatives are 17.1 and 10.7 wt %, respectively [1]. In spite of serious trimethylsilylation, therefore, only half of the OH groups are grafted, which is possibly

TABLE II BET specific surface areas ($m^2 g^{-1}$) of CTSH, CHA and PTSH before and after heating in nitrogen and air

HTT (K)	CTSH		CHA		PTSH*	
	N_2	Air	N_2	Air	N_2	Air
Original	490		420		250	
473	500	500	420	430	250	260
673	560	650	410	410	380	370
873	750	500	410	400	340	340
1073	480	330	370	350	270	180
1273	310	10	260	280	30	20
1473	†	†	†	†	10	†

*The partially trimethylsilylated halloysite. Raw HA 110 $m^2 g^{-1}$; raw HA after heating to 673 K in nitrogen 80 $m^2 g^{-1}$.
†Too small to measure.

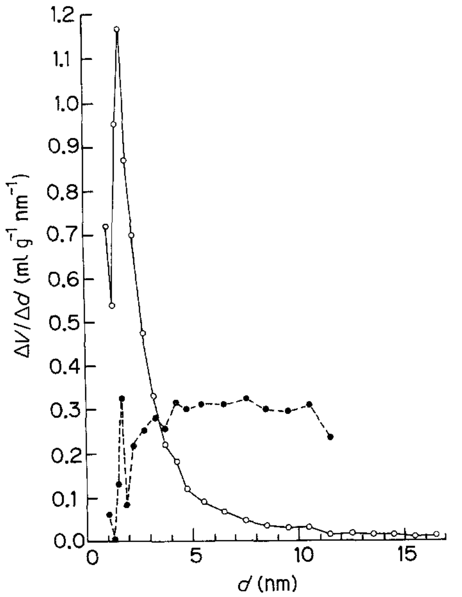

Figure 6 Pore-size distribution diagrams of (○) CTSH and (●) CHA before heating.

attributable to the steric hindrance of the bulky trimethylsilyl group as described by Kuroda and Kato [1].

It is apparent from the results of infrared spectra, carbon content and specific surface area that the original structure of the CTSH remains unchanged up to 473 K in both atmospheres. Above 673 K, the thermal behaviour of CTSH is influenced by the heat-treatment atmosphere, i.e. the CTSH undergoes combustion in air at this HTT resulting in a reduction of the carbon content to one-half, in contrast to slight structural change in nitrogen as shown by very small changes of analytical data. The exothermic weight decrease of the CTSH was observed at 673 K (Fig. 4). This discrepancy may be considered as follows: the TG–DTA curves were taken on a steady heating process, in contrast to the 1 h residence used for the sample when measuring carbon content. Because the surface area increased after this structural change with decrease of carbon content, the removal of the $-CH_3$ group must leave the $-Si-O-$ pillar cross-linked between the Si–O tetrahedron sheets.

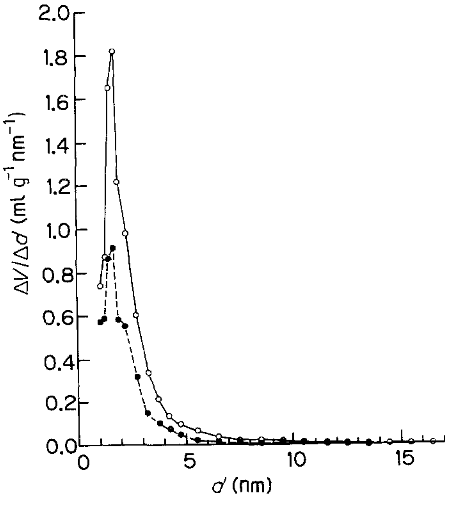

Figure 7 Pore-size distribution diagrams of CTSH after heating to 873 K in (○) nitrogen and (●) air.

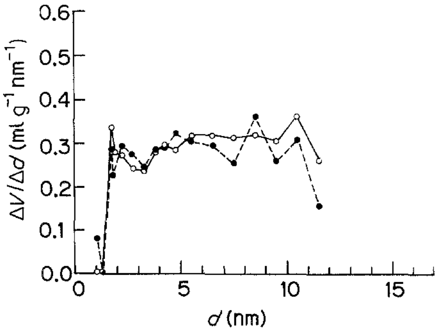

Figure 8 Pore-size distribution diagrams of CHA after heating to 873 K in (○) nitrogen and (●) air.

Heating to 873 K in nitrogen brought about a decrease in carbon content, a weakening of infrared absorptions assigned to $-CH_3$ and the endothermic weight decrease (though not presented here), all indicating the removal of $-CH_3$. The surface area of CTSH is also increased after these structural changes. After heating to 873 K in air, however, the porous structure begins to sinter because of the decrease in surface area. As suggested from these discussions, $-CH_3$ is effective in inhibiting sintering between the Si–O tetrahedron sheets, leading to the retention of a large surface area. We have reported similar phenomena using the montmorillonite/naphthylamine complex [3] and the saponite/naphthylamine complex [4].

Even after heating to 1073 K in nitrogen, 6.6 wt % carbon remains, some of which results from $-CH_3$, a little of which remains from infrared absorptions assigned to $-CH_3$. The remaining $-CH_3$ group still contributes to the retention of a large surface area. After heating to 1273 K in both nitrogen and air, the surface areas are 300 m^2 g^{-1} and just 10 m^2 g^{-1}, respectively. The former sample contains 5 wt % carbon but the absorptions assigned to $-CH_3$ disappeared completely. The state of the remaining carbon is not clear, but such carbon also contributes to the

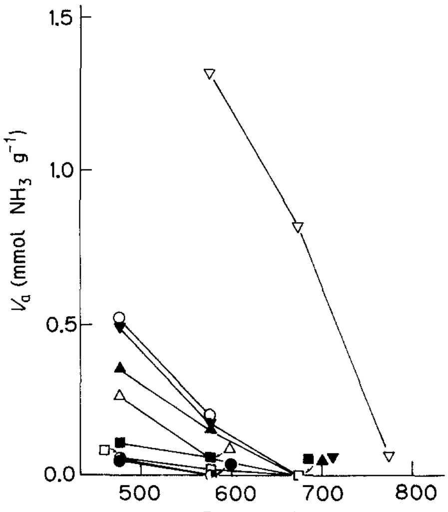

Figure 9 Comparison of acidic properties of raw HA, some derivatives after heating and some commercially available catalysts. (○) Raw HA; (◑) CTSH, 673 K, air; (●) CTSH, 873 K, air; (□) CHA, 673 K, air; (■) CHA, 673 K, nitrogen; (△) PTSH, 673 K, nitrogen; (▽) Zeolon 100 H (Norton); (▲) JRC-ALO-I; (▼) N-631L (Nikki).

retention of a large surface area even at such a high HTT. However, the CTSH porous structure sinters considerably after heating to 1273 K in air. At 1473 K, the CTSH sinters completely to crystallize into cristobalite regardless of heat-treatment atmosphere.

4.2. Thermal degradation behaviour of CHA

CHA appears to have the structure shown in Fig. 1, in view of the strong absorptions assigned to –OH group and the presence of no or just a little aluminium as suggested from the formation of cristobalite. It is also reasonable, from the formation of the resulting non-rigid Si–O tetrahedron sheet, to consider that CHA is an amorphous material. CHA consists of a relatively rough porous structure, as suggested from its broad pore-size distribution diagram in which the relatively large pores are included. Therefore, pores may be formed among the wrinkled Si–O tetrahedron sheets.

The atmosphere has no effect on the thermal degradation behaviour of CHA possibly because of the absence of carbon. Infrared spectra suggest that the structure of CHA remains unchanged up to 873 K, which is highly consistent with no change in the specific surface area in this temperature range. The weight decrease around 400 K (Fig. 5), therefore, results from the removal of adsorbed water. When HTT reaches 873 K, the CHA porous structure begins to sinter, as suggested from the decrease in surface area. The surface area of the CHA decreased more slowly with increasing HTT than in PTSH and CTSH. It may be that the CHA includes larger pores which hinder sintering.

4.3. Evaluation of the CTSH as a thermally stable porous material

The CTSH has a larger surface area than the PTSH but both samples are very similar in other properties. In the previous paper [2], the PTSH porous material was compared with zeolite and the pillared interlayered clay (PILC) (e.g. [5]), although the details are not described here.

The CTSH porous material is characterized by an amorphous state including the extremely homogeneous porous structure resulting from the grafted trimethylsilyl group. It is not easy to evaluate this amorphous state to the crystalline structure of zeolite and the layer structure of PILC. However, one of the main purposes in preparing PILC was to obtain a thermally stable porous material which included larger homogeneous pores than those in zeolite, even if the resulting material had no layer structure. These demands are also satisfied by CTSH. In addition, CTSH has a higher thermal stability than PILC. This discussion suggests that the CTSH porous material is a promising material, although it cannot be used as a catalyst in view of its poor acidic property.

Acknowledgements

The authors wish to thank Mr Y. Tsurita of Mitsubishi Chemical Ind. for acidic property measurements and Mr H. Hanaoka of Gunmaken Industrial Research Laboratory for the carbon content measurements.

References

1. K. KURODA and C. KATO, *Clays Clay Minerals* **27** (1979) 53.
2. A. ŌYA, K. KIZU and S. ŌTANI, *Appl. Clay Sci.*, submitted.
3. A. ŌYA, Y. OMATA and S. ŌTANI, *J. Mater. Sci.* **20** (1985) 255.
4. *Idem, Amer. Ceram. Soc. Bull.* **65** (1986) 776.
5. T. J. PINNAVAIA, *Science* **220** (1983) 365.

Received 9 March
and accepted 15 May 1987